JAERI-M
92-064

BOOTSTRAP CURRENT PROFILES AND SCALING IN LARGE ASPECT RATIO TOKAMAKS

May 1992

Noboru FUJISAWA and Tomonori TAKIZUKA

日 本 原 子 力 研 究 所
Japan Atomic Energy Research Institute

JAERI-Mレポートは，日本原子力研究所が不定期に公刊している研究報告書です。
入手の問合わせは，日本原子力研究所技術情報部情報資料課（〒319－11茨城県那珂郡東海村）あて，お申しこしください。なお，このほかに財団法人原子力弘済会資料センター（〒319-11茨城県那珂郡東海村日本原子力研究所内）で複写による実費頒布をおこなっております。

JAERI-M reports are issued irregularly.
Inquiries about availability of the reports should be addressed to Information Division, Department of Technical Information, Japan Atomic Energy Research Institute, Tokai-mura, Naka-gun, Ibaraki-ken 319-11, Japan.

編集兼発行　日本原子力研究所
印　　刷　日立高速印刷株式会社

JAERI-M 92-064

Bootstrap Current Profiles and Scaling in Large Aspect Ratio Tokamaks

Noboru FUJISAWA and Tomonori TAKIZUKA[+]

Fusion Experimental Reactor Team
Naka Fusion Research Establishment
Japan Atomic Energy Research Institute
Naka-machi, Naka-gun, Ibaraki-ken

(Received April 8, 1992)

Recently, bootstrap currents, generated spontaneously in a tokamak plasma, have been observed in large tokamak devices. Those bootstrap currents are applied to designs of a next-generation experimental tokamak reactor like ITER and following tokamak power reactors. In those designs, with enhancing a fraction of the bootstrap current to the total plasma current, which reduces the power for current drive, the power flowing out from a plasma and into a divertor plate is substantially reduced and resultantly the issue on the divertor is alleviated to some extent. At the same time the bootstrap current enhances the Q-value of tokamak reactors.

The bootstrap current intrinsically has a hollow profile. With increasing the fraction of the bootstrap current, a bootstrap current density is frequently beyond a total current density somewhere in a plasma radius, which is not preferable from the view point of an extemal current drive. For a tokamak with a large aspect ratio, a current density profile externally supplied is studied in an interesting range of total plasma current density and pressure profiles, and preferable profiles of current and pressure are identified. A peaked profile for the pressure and a hollow profile for the current are desirable.

A simple expression for a bootstrap current of a tokamak with a large aspect ratio is proposed, which can easily evaluate the bootstrap

current. Some empirical scalings for a bootstrap current with a finite aspect ratio have been proposed so far, and the applicability of them is briefly discussed.

Keywords : Bootstrap Current, Current Drive, ITER

JAERI－M 92－064

大アスペクト比トカマクのブートストラップ電流の分布とスケーリング

日本原子力研究所那珂研究所核融合実験炉特別チーム
藤沢　登・滝塚　知典[+]

（1992年4月8日受理）

最近，トカマクプラズマ中に自発的に誘起されるブートストラップ電流が大型トカマク装置の実験で観測されるようになり，ITER等の次期トカマク実験炉やトカマク型動力炉などの設計に積極的に取り入れられるようになった。これらの設計ではブートストラップ電流の全体に占める割合を大きくすることにより，電流駆動パワーを大幅に減らし，プラズマから流出しダイバータへ流れ込むパワーを小さくし，ダイバータでの熱処理の問題を楽にすると同時に，トカマク型核融合炉のQ値を上げている。

ブートストラップ電流密度は本質的にホローな径方向分布となるため，ブートストラップ電流を大きくしていくと，しばしばその電流密度が全電流密度を越えてしまう様な極端な分布が生じる。大きなアスペクト比のトカマクについて，全プラズマ電流密度とプラズマ圧力の分布について外部から供給すべき電流密度の分布を求め，好ましい電流密度と圧力の分布を調べた。全プラズマ電流密度分布はできるだけフラットな，プラズマの圧力についてはできるだけピークした分布が適切である。

大アスペクト比トカマクのブートストラップ電流を簡単に求めることができる表式を求めた。有限のアスペクト比についてはいくつか経験的な表式が提案されているが，その表式の有用性について簡単な議論をする。

那珂研究所：〒311－01 茨城県那珂郡那珂町大字向山801－1
＋　炉心プラズマ研究部

Contents

目　　次

1. Introduction

A bootstrap current will play a significant role in future tokamak reactors, such as a next-generation experimental tokamak reactor like ITER[1] and power reactors, such as SSTR[2] and ARIES[3]. In those tokamaks, handling of large power, including fusion alpha heating power and externally supplied powers for current drive and burn control, which flows out from a plasma and enters mainly onto a divertor plate, is a crucial issue, being left to be successfully solved so far. In particular, steady state operation in those tokamaks needs a substantial power for non-inductive current drive, which is added to an alpha heating power, and the total heating power remarkably increases. The use of the large bootstrap current alleviates the problem to some degree by reducing the power required for non-inductive current drive. Power reactor studies show that the reduction of current drive power due to a large fraction of bootstrap current not only reduces the power to be extracted from a divertor, but also enhances a power multiplication factor of a tokamak reactor up to a reasonable level, e.g., up to ~30. Without making use of the large bootstrap current, a tokamak reactor could not compete with other energy resources.

In design studies of tokamak reactors such as experimental tokamak reactors and power reactors, a systematic survey, using a zero-dimensional model, has been made to select a preferable set of device parameters in certain conditions. As mentioned above, the bootstrap current has a considerable impact on the survey. However no simple formula of the bootstrap current has been established yet, although the bootstrap current can be accurately evaluated in a two-dimensional model, which is not convenient to a simple model. Some empirical formula have been proposed [4, 5, 6], but their applicability and accuracy have not yet been identified. In this paper, a simple expression for the bootstrap current in an infinitely large-aspect-ratio tokamak is derived on the basis of the theoretical formula given in [7].

The use of a large fraction of the bootstrap current is a reasonable tendency in designing future tokamaks. The bootstrap current has intrinsically a hollow profile, and the introduction of a large fraction of the bootstrap current may distort a profile of a total parallel current density. A source current externally supplied by a current drive system is studied in this paper from a viewpoint of what profiles of pressure and current density produce a preferable bootstrap current profile.

2. Numerical fit to bootstrap currents of tokamaks with a large aspect ratio

A bootstrap current density in a large-aspect-ratio tokamak is analytically expressed as [7],

$$j_{bs}(r) = \sqrt{\frac{r}{R}}\,\frac{p_e}{B_\theta}\left\{ -4.88\,\frac{1}{n}\frac{\partial n}{\partial r} - 0.27\,\frac{1}{T}\frac{\partial T}{\partial r} \right\}, \qquad (1)$$

where r is a radial coordinate for a minor plasma radius, R is a major radius, p_e is electron pressure, B_θ is a poloidal component of magnetic field, n and T are plasma density and temperature in which ion and electron are assumed to have equal density and temperature.

1. Introduction

A bootstrap current will play a significant role in future tokamak reactors, such as a next-generation experimental tokamak reactor like ITER[1] and power reactors, such as SSTR[2] and ARIES[3]. In those tokamaks, handling of large power, including fusion alpha heating power and externally supplied powers for current drive and burn control, which flows out from a plasma and enters mainly onto a divertor plate, is a crucial issue, being left to be successfully solved so far. In particular, steady state operation in those tokamaks needs a substantial power for non-inductive current drive, which is added to an alpha heating power, and the total heating power remarkably increases. The use of the large bootstrap current alleviates the problem to some degree by reducing the power required for non-inductive current drive. Power reactor studies show that the reduction of current drive power due to a large fraction of bootstrap current not only reduces the power to be extracted from a divertor, but also enhances a power multiplication factor of a tokamak reactor up to a reasonable level, e.g., up to ~30. Without making use of the large bootstrap current, a tokamak reactor could not compete with other energy resources.

In design studies of tokamak reactors such as experimental tokamak reactors and power reactors, a systematic survey, using a zero-dimensional model, has been made to select a preferable set of device parameters in certain conditions. As mentioned above, the bootstrap current has a considerable impact on the survey. However no simple formula of the bootstrap current has been established yet, although the bootstrap current can be accurately evaluated in a two-dimensional model, which is not convenient to a simple model. Some empirical formula have been proposed [4, 5, 6], but their applicability and accuracy have not yet been identified. In this paper, a simple expression for the bootstrap current in an infinitely large-aspect-ratio tokamak is derived on the basis of the theoretical formula given in [7].

The use of a large fraction of the bootstrap current is a reasonable tendency in designing future tokamaks. The bootstrap current has intrinsically a hollow profile, and the introduction of a large fraction of the bootstrap current may distort a profile of a total parallel current density. A source current externally supplied by a current drive system is studied in this paper from a viewpoint of what profiles of pressure and current density produce a preferable bootstrap current profile.

2. Numerical fit to bootstrap currents of tokamaks with a large aspect ratio

A bootstrap current density in a large-aspect-ratio tokamak is analytically expressed as [7],

$$j_{bs}(r) = \sqrt{\frac{r}{R}}\,\frac{p_e}{B_\theta}\left\{ -4.88\,\frac{1}{n}\frac{\partial n}{\partial r} - 0.27\,\frac{1}{T}\frac{\partial T}{\partial r} \right\}, \qquad (1)$$

where r is a radial coordinate for a minor plasma radius, R is a major radius, p_e is electron pressure, B_θ is a poloidal component of magnetic field, n and T are plasma density and temperature in which ion and electron are assumed to have equal density and temperature.

Assuming that constant flux surfaces have approximately concentric circular cross sections, and those profiles of pressure, temperature and total parallel current density have the forms of

$$H = H_0 \left(1 - x^2\right)^{\alpha_H} , \tag{2}$$

where H represents pressure (P), temperature (T) and current density (J) and x=r/a, the bootstrap current density normalized by an average current density leads to

$$\frac{\pi a^2}{I_P} j_{bs}(x) = \sqrt{\varepsilon}\, \beta_p \left(1.22 - 1.15 \frac{\alpha_T}{\alpha_P}\right) \alpha_P (\alpha_P + 1) \frac{x^{5/2}\left(1 - x^2\right)^{\alpha_P - 1}}{1 - \left(1 - x^2\right)^{\alpha_J + 1}} , \tag{3}$$

where ε=a/R and I_P are the aspect ratio and total (parallel) plasma current, respectively, and a poloidal beta is defined as $\beta_P = 2\mu_0 p/B_a^2$ (p and B_a are the total pressure and poloidal magnetic field at r=a). Therefore the total bootstrap current normalized by $\sqrt{\varepsilon}\beta_P I_P$ is expressed as follows;

$$\frac{I_{bs}}{\sqrt{\varepsilon}\beta_p I_p} = \left(1.22 - 1.15 \frac{\alpha_T}{\alpha_P}\right) F(\alpha_P, \alpha_J) , \tag{4}$$

$$F(\alpha_P, \alpha_J) = \alpha_P (\alpha_P + 1) \int_0^1 \frac{y^{5/4}(1 - y)^{\alpha_P - 1}}{1 - (1 - y)^{\alpha_J + 1}} dy . \tag{5}$$

The function $F(\alpha_P, \alpha_J)$ is numerically evaluated in interesting ranges of α_P and α_J, and the results are shown in Fig.1. The closed circles in Fig.1 are the numerical results of $F(\alpha_P, \alpha_J)$. The function $F(\alpha_P, \alpha_J)$ increases almost linearly with α_P, especially in a region of small α_J. The total bootstrap current has strong dependence upon α_J, namely the bootstrap current can be maximized with peaked pressure and flat current profiles. Especially a flat current profile significantly enhances a bootstrap current, where the peaked pressure profile also increases a bootstrap current. On the other hand, for a peaked parallel current profile, e.g. $\alpha_J \geq 1.5$, the total bootstrap current has little dependence on α_P and makes a small contribution to the total current.

The function $F(\alpha_P, \alpha_J)$ can be approximated adequately with the following fitting function, which is shown as solid lines in Fig.1;

$$F(\alpha_P, \alpha_J) = \frac{0.90635}{1 + \alpha_J} \left\{ \left(\frac{1 + \alpha_J}{0.90635} \right)^{4/3} + \alpha_P \frac{\alpha_P + C_1(\alpha_J)}{\alpha_P + C_2(\alpha_J)} \right\}^{3/4} , \tag{6}$$

$$C_1(\alpha_J) = 0.85334 - 0.31958\alpha_J - 0.21981\alpha_J^2 + 0.0095504\alpha_J^3 , \tag{6a}$$

$$C_2(\alpha_J) = 0.85126 - 0.44094\alpha_J - 0.024996\alpha_J^2 + 0.000070467\alpha_J^3 . \tag{6b}$$

A form of the fitting function is selected by considering the following analytical relations;

$$F(\alpha_P \to \infty, \alpha_J) = \frac{0.90635}{1+\alpha_J}\alpha_P^{3/4} , \tag{7a}$$

$$F(\alpha_P \to 0, \alpha_J) = 1 + f(\alpha_J)\,\alpha_P . \tag{7b}$$

The relative error is within ±1% for wide ranges of $0<\alpha_P, \alpha_J<10$.

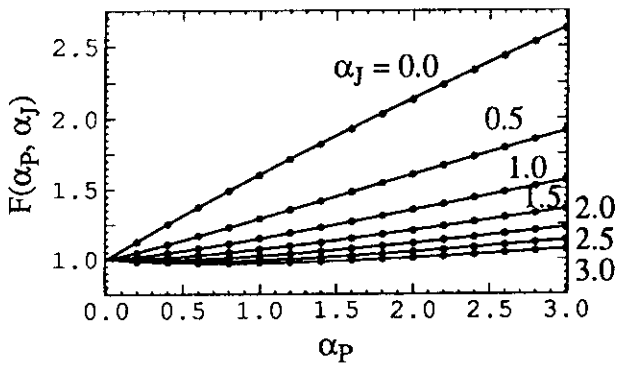

Fig.1 Numerical results of $F(\alpha_P, \alpha_J)$ and their fitting functions. Numerical results of $F(\alpha_P, \alpha_J)$ are shown as closed circles and the fitting function of Eq.(6) are plotted with solid lines. The horizontal axis is an exponent of a parabolic pressure profile, α_P, and α_J, varied as a parameter from 0.0 to 3.0, is an exponent of a parabolic current density profile.

3. Bootstrap current profiles

The use of a large fraction of bootstrap current is attractive, probably indispensable, for future tokamak reactors. The large fraction of bootstrap current can reduce an necessary current drive power, which resultantly decreases the power to be handled at a divertor plate. Since a bootstrap current has intrinsically a hollow profile, a large bootstrap current fraction tends to require a strange profile of an external source current. In an extreme case, it requires a negative source current somewhere in a plasma minor radius, which does not help reducing current drive power, and such an extreme case should be avoided in designing tokamak reactors. In this section, we study desirable profiles of pressure and total current density with using a simple model of a tokamak with a circular cross section for a large aspect ratio, which is discussed in the previous section to some extent.

Using the above expression of the numerical fit to the total bootstrap current, the bootstrap current density, normalized by the average parallel current density, can be written as follows.

A form of the fitting function is selected by considering the following analytical relations;

$$F(\alpha_P \to \infty, \alpha_J) = \frac{0.90635}{1+\alpha_J}\alpha_P^{3/4} , \tag{7a}$$

$$F(\alpha_P \to 0, \alpha_J) = 1 + f(\alpha_J)\,\alpha_P . \tag{7b}$$

The relative error is within ±1% for wide ranges of $0<\alpha_P, \alpha_J<10$.

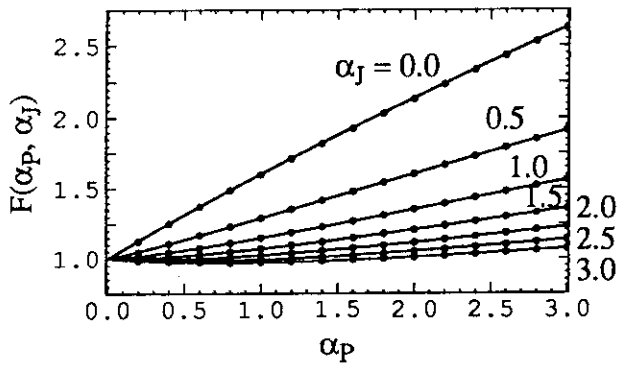

Fig.1 Numerical results of $F(\alpha_P, \alpha_J)$ and their fitting functions. Numerical results of $F(\alpha_P, \alpha_J)$ are shown as closed circles and the fitting function of Eq.(6) are plotted with solid lines. The horizontal axis is an exponent of a parabolic pressure profile,α_P, and α_J, varied as a parameter from 0.0 to 3.0, is an exponent of a parabolic current density profile.

3. Bootstrap current profiles

The use of a large fraction of bootstrap current is attractive, probably indispensable, for future tokamak reactors. The large fraction of bootstrap current can reduce an necessary current drive power, which resultantly decreases the power to be handled at a divertor plate. Since a bootstrap current has intrinsically a hollow profile, a large bootstrap current fraction tends to require a strange profile of an external source current. In an extreme case, it requires a negative source current somewhere in a plasma minor radius, which does not help reducing current drive power, and such an extreme case should be avoided in designing tokamak reactors. In this section, we study desirable profiles of pressure and total current density with using a simple model of a tokamak with a circular cross section for a large aspect ratio, which is discussed in the previous section to some extent.

Using the above expression of the numerical fit to the total bootstrap current, the bootstrap current density, normalized by the average parallel current density, can be written as follows.

$$\frac{\pi a^2}{I_P} j_{bs}(x) = \frac{I_{bs}}{I_P} \frac{\alpha_P(\alpha_P + 1)}{F(\alpha_P, \alpha_J)} \frac{x^{5/2}(1 - x^2)^{\alpha_P - 1}}{1 - (1 - x^2)^{\alpha_J + 1}} . \tag{8}$$

Typical profiles of bootstrap current are shown in Fig.2. The profile of the bootstrap current is mainly depend on α_P. With decreasing α_P, the peak of the bootstrap current, which appears near the plasma axis at a large α_P, moves to the plasma edge, and in the region of $\alpha_P \leq 1.0$ the peak appears on the plasma boundary. Therefore the bootstrap current density in the range of small α_P tends to exceed the parallel total current density in the plasma edge region, where a negative external source current has to be driven to compensate a bootstrap current, to maintain a ordinary parallel current profile.

The external source current density, $j_{es}(x)$, defined as a difference between the total parallel and bootstrap current densities, is expressed as

$$j_{es}(x) = j_t(x) - j_{bs}(x) . \tag{9}$$

Since the normalized bootstrap current can be expressed with I_{bs}/I_p, α_P, and α_J, as Eq.(8), the external source current density, normalized by the average parallel current density, also depends on the fraction of bootstrap current, I_{bs}/I_p, and the profile indicators of pressure and current, α_P and α_J.

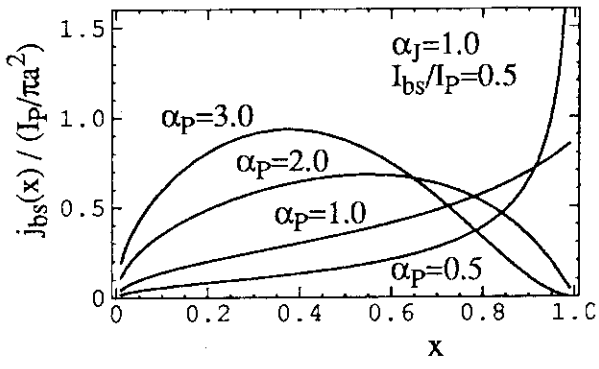

Fig.2 Bootstrap current density profiles, normalized with an average parallel current density. The parallel current profile is parabolic with an exponent α_J=1.0, and the fraction of bootstrap current is 50%. The profile of pressure is varied from peaked (α_P=3.0) to flat (α_P=0.5).

The equi-contours of the minimum external source current density are shown in the plane of α_P and α_J as a parameter of the fraction of bootstrap current, I_{bs}/I_p, in Fig.3. As mentioned previously, in the region of $\alpha_P \leq 1.0$ the peak of the bootstrap current density appears at plasma edge and the external source current density becomes negative there. Generally speaking, in the upper-left region of the α_P-α_J plane the minimum of the external source current is negative and in the lower-right region the minimum becomes positive, which

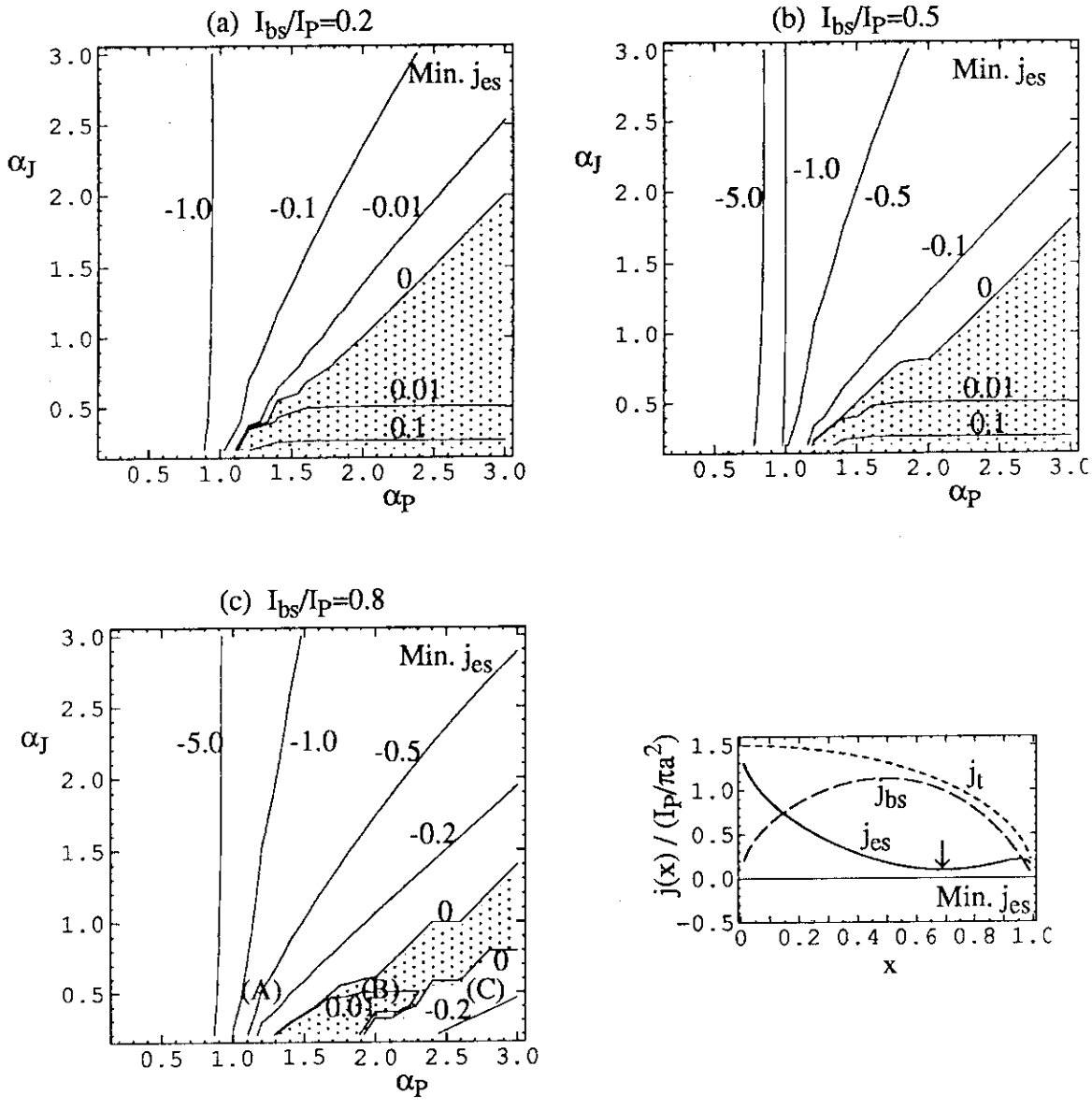

Fig.3 Contour plot of the minimum of external source current density, normalized by an average parallel current density, in the α_P-α_J plane. Figures (a), (b) and (c) correspond to cases with the fraction of bootstrap current I_{bs}/I_P of 0.2, 0.5, and 0.8, respectively. In dotted spaces, shown in (a), (b) and (c), the minimum external current density is positive, as shown in the lower-right figure for profiles of current densities, where the arrow shows the minimum of the external source current density.

is shown as dotted regions in Fig.3. With increasing the fraction of bootstrap current, however, the negative region appears again in the lower-right corner, and the region of the positive minimum is narrowed down, as shown in Fig.3(c). In the negative external current density region reappearing in the lower-right corner for the higher fraction of the bootstrap current, the peak of the bootstrap current density exceeds the parallel current density in the middle of a plasma radius, as shown in Fig.4(C). Figures 4 shows typical profiles of the total, bootstrap and external source current densities for representative regions in the α_P-α_J plane of Fig.3 (c).

The fraction of the total negative external source current to the total current, defined as

$$\frac{I_{es,\,n}}{I_P} = \frac{1}{I_P}\int j_{es}\,|_{\,negative}\,dS\ , \tag{10}$$

is also plotted in Fig. 5. The general tendency is similar to Fig. 3. In the lower-right corner, shown as dotted areas, the external source current density has no negative values, which seems desirable for current driven externally. In the most of α_P-α_J space the external source current density has negative current, especially in the upper-left regions the negative current increases. In the region of $\alpha_P \leq 1.0$ the negative external current always appears, because the bootstrap current peaks at a plasma edge, as mentioned above. To avoid somewhat complicated profile of the external current the regions with higher α_P and lower α_J should be selected.

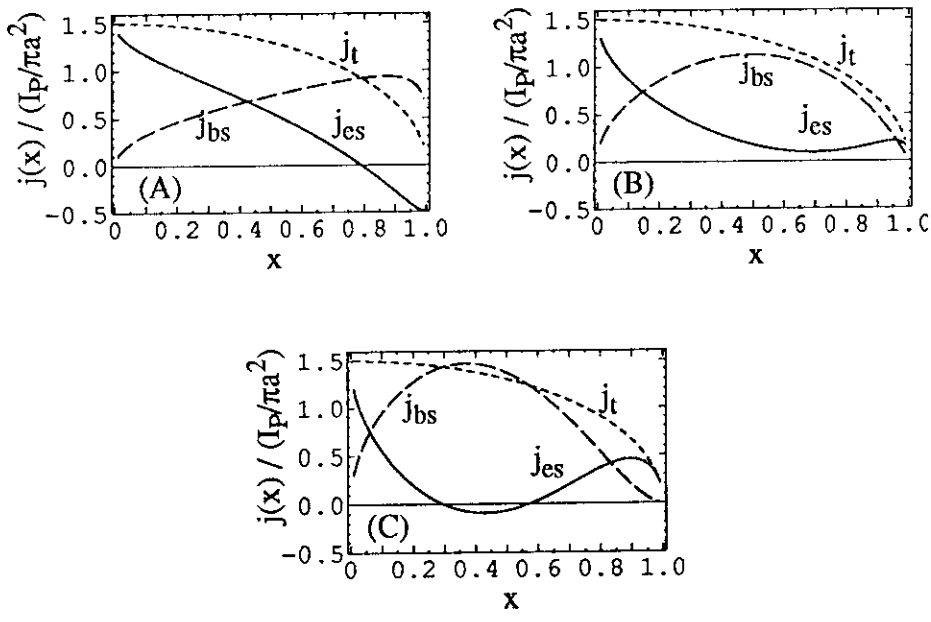

Fig.4 Typical profiles of total parallel current density j_t, bootstrap current density j_{bs}, and external source current density j_{es} at positions indicated in Fig.3 (c). I_{bs}/I_P=0.8, α_J=0.5, and α_P=1.2, 2.0, and 2.8 correspond to (A), (B), and (C), respectively.

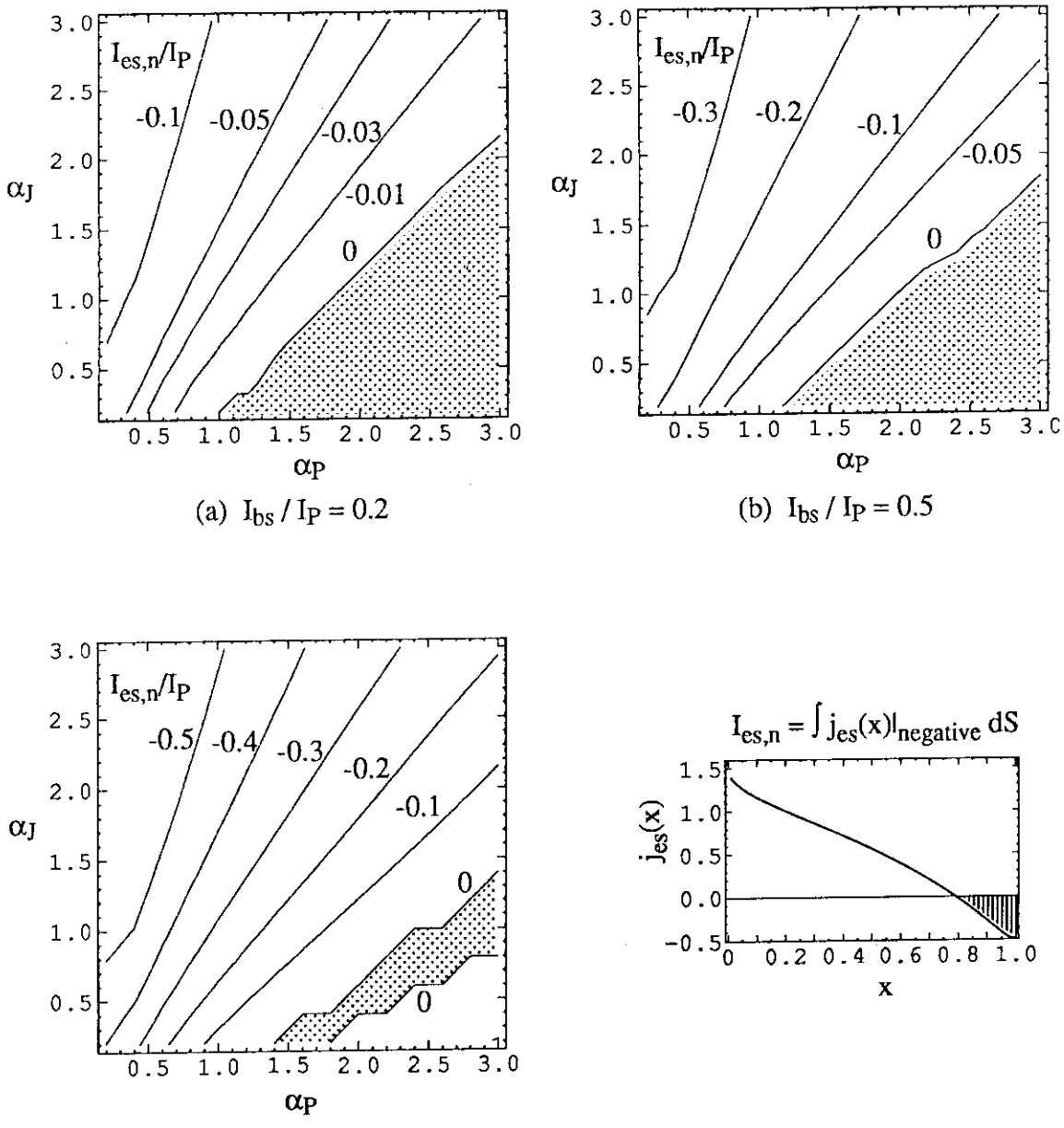

Fig.5 Contour plots of integrated negative external source current, normalized with the total parallel current, in the α_P-α_J plane. The integrated area is hatched in the lower-right corner of the figure. Figure (a), (b) and (c) corresponds to the fraction of bootstrap current of 0.2, 0.5 and 0.8, respectively. In the dotted regions of the contour plots the external source current density is always positive.

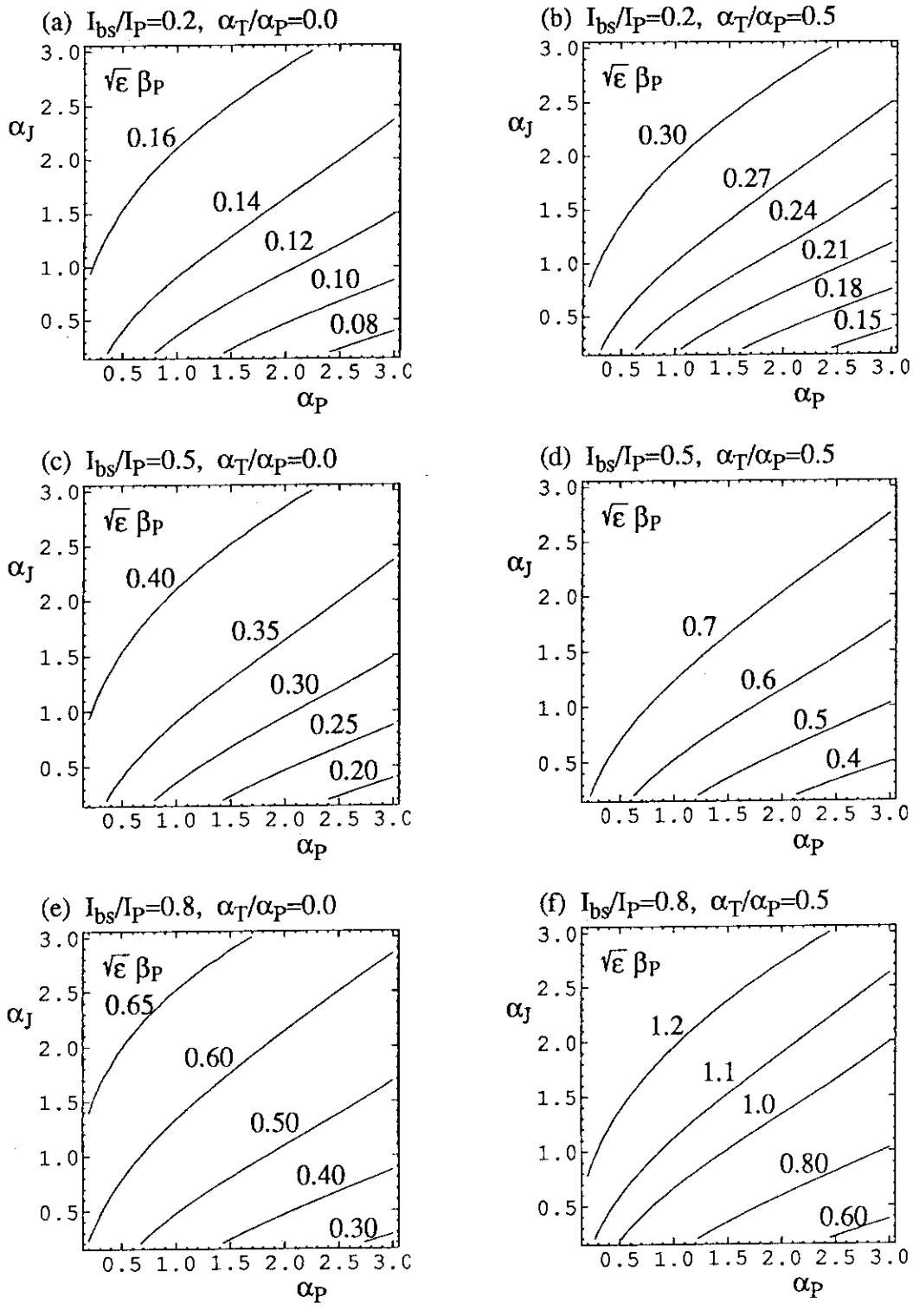

Fig.6 Contour plots of $\sqrt{\varepsilon}\beta_P$ in the α_T-α_J plane, required to generate the bootstrap current fraction, I_{bs}/I_P=0.2, 0.5 and 0.8, for the ratio of temperature and pressure profile, α_T/α_P=0.0 and 0.5.

The value of $\sqrt{\varepsilon}\beta_P$ to generate the given fraction of bootstrap current is also evaluated in the α_P-α_J plane as a parameter of a ratio of α_T and α_P, as shown in Fig. 6. The $\sqrt{\varepsilon}\beta_P$ decreases with moving from the upper-left corner to the lower-right corner. It reflects the favourable tendencies of α_P and α_J to the bootstrap current. For the same pressure profile the case of α_T=0 requires the smallest value, namely a peaked density and flat temperature profile produces the larger bootstrap current for the same plasma poloidal beta. For I_{bs}/I_P=0.8, the necessary $\sqrt{\varepsilon}\beta_P$ is 0.4~0.8, which correspond to β_P=0.8~1.6 for ε=0.25 (aspect ratio, A=4). Those poloidal beta values are not unrealistic.

From the above results, the favourable condition for producing a reasonably substantial bootstrap current is a flat parallel current (small α_J) and a peaked pressure profile (large α_P), which should have a peaked density profile and a flat temperature profile (small α_T). The flat profile of the total parallel current density may be produced with an appropriate external current drive, because the large bootstrap current tends to be hollow. The issue is how to make the pressure profile peaked, especially peaked density and flat temperature profile. It is strongly coupled with transport of power and particle, and it may be difficult to control them externally.

4. Comparison of empirical scalings for a finite aspect ratio

The following empirical fit of bootstrap currents for a finite aspect ratio was proposed by one of the authors, based on a lot of numerical results of two-dimensional equilibria for ITER with variety of profiles of density, temperature, and parallel current density, and changing plasma pressure, effective charge, impurity species, except for an almost fixed aspect ratio [4];

$$\frac{I_{bs}}{I_P} = C_{bs}\left(\sqrt{\varepsilon}\,\beta_P\right)^{1.3} , \tag{11}$$

$$C_{bs} = 1.32 - 0.235\left[\frac{q_\psi(95\%)}{q_\psi(0)}\right] + 0.0185\left[\frac{q_\psi(95\%)}{q_\psi(0)}\right]^2 , \tag{11a}$$

where $q_\psi(0)$ and $q_\psi(95\%)$ are safety factors at a plasma center and at a 95% magnetic flux surface, respectively. It suggests that the bootstrap current depends mainly upon the profile of total parallel current, in addition to the dependence of β_P, as mentioned in the previous section. The expression suggests the weak dependence of I_{bs}/I_P on the profiles of pressure and temperature, while the former expression of Eq.(4) shows the strong dependence on those profiles. The difference should be disclosed, taking into account of the effect of finite aspect ratio. The strong dependence of the bootstrap current on the current profile could be due to change of magnetic flux surfaces [5]. This tendency can be seen from the following expression of the bootstrap current,

$$I_{bs} = \int d\psi\, q(\psi)\frac{\langle\langle \mathbf{B}\cdot\mathbf{J}\rangle\rangle_{bs}}{\langle\langle \mathbf{B}^2\rangle\rangle} , \tag{12}$$

The value of $\sqrt{\varepsilon}\beta_P$ to generate the given fraction of bootstrap current is also evaluated in the α_P-α_J plane as a parameter of a ratio of α_T and α_P, as shown in Fig. 6. The $\sqrt{\varepsilon}\beta_P$ decreases with moving from the upper-left corner to the lower-right corner. It reflects the favourable tendencies of α_P and α_J to the bootstrap current. For the same pressure profile the case of α_T=0 requires the smallest value, namely a peaked density and flat temperature profile produces the larger bootstrap current for the same plasma poloidal beta. For I_{bs}/I_P=0.8, the necessary $\sqrt{\varepsilon}\beta_P$ is 0.4~0.8, which correspond to β_P=0.8~1.6 for ε=0.25 (aspect ratio, A=4). Those poloidal beta values are not unrealistic.

From the above results, the favourable condition for producing a reasonably substantial bootstrap current is a flat parallel current (small α_J) and a peaked pressure profile (large α_P), which should have a peaked density profile and a flat temperature profile (small α_T). The flat profile of the total parallel current density may be produced with an appropriate external current drive, because the large bootstrap current tends to be hollow. The issue is how to make the pressure profile peaked, especially peaked density and flat temperature profile. It is strongly coupled with transport of power and particle, and it may be difficult to control them externally.

4. Comparison of empirical scalings for a finite aspect ratio

The following empirical fit of bootstrap currents for a finite aspect ratio was proposed by one of the authors, based on a lot of numerical results of two-dimensional equilibria for ITER with variety of profiles of density, temperature, and parallel current density, and changing plasma pressure, effective charge, impurity species, except for an almost fixed aspect ratio [4];

$$\frac{I_{bs}}{I_P} = C_{bs}\left(\sqrt{\varepsilon}\,\beta_P\right)^{1.3} , \tag{11}$$

$$C_{bs} = 1.32 - 0.235\left[\frac{q_\psi(95\%)}{q_\psi(0)}\right] + 0.0185\left[\frac{q_\psi(95\%)}{q_\psi(0)}\right]^2 , \tag{11a}$$

where $q_\psi(0)$ and $q_\psi(95\%)$ are safety factors at a plasma center and at a 95% magnetic flux surface, respectively. It suggests that the bootstrap current depends mainly upon the profile of total parallel current, in addition to the dependence of β_P, as mentioned in the previous section. The expression suggests the weak dependence of I_{bs}/I_P on the profiles of pressure and temperature, while the former expression of Eq.(4) shows the strong dependence on those profiles. The difference should be disclosed, taking into account of the effect of finite aspect ratio. The strong dependence of the bootstrap current on the current profile could be due to change of magnetic flux surfaces [5]. This tendency can be seen from the following expression of the bootstrap current,

$$I_{bs} = \int d\psi\, q(\psi)\frac{\langle\langle \mathbf{B}\cdot\mathbf{J}\rangle\rangle_{bs}}{\langle\langle \mathbf{B}^2\rangle\rangle} , \tag{12}$$

where $\langle\langle\ \rangle\rangle$ refers to a flux average and $\langle\langle \mathbf{B}\cdot\mathbf{J}\rangle\rangle_{bs}$ is the bootstrap current. The area factor comes from the q dependence. It was also pointed out [5] that the exponent of 1.3 of $\sqrt{\varepsilon}\beta_P$ is somewhat high and that a formula using an internal inductance might be more preferable to express a numerical fit than the ratio of q_ψ's.

Recently the scaling of bootstrap currents with an arbitrary aspect ratio was also studied in [6]. The following expression for the bootstrap current was proposed from the empirical fit of about 3000 numerical solutions of two-dimensional equilibria, including various aspect ratios, profiles of pressure, temperature and current, and effective charge (Z);

$$\frac{I_{bs}}{\sqrt{\varepsilon}\beta_P I_P} = \sum_{i=1}^{12} a_i(\alpha_J, Z)\ b_i(\alpha_P, \alpha_T, \varepsilon)\ . \tag{12}$$

It was noted there that the above scaling of the bootstrap current reproduces reasonably well the numerical solution of bootstrap current in the large aspect ratio limit. In Fig. 7, the proposed scaling is compared with the numerical solution for a large aspect ratio limit, described in the previous section. In the reference [6], only a case of α_P=3.0 is compared and it is concluded that the reasonable agreement is reproduced, as plotted in the figure. Obviously seen in the figure, however, large differences are observed between the scaling and the numerical solution, especially in the cases of small α_P. It is not clear so far the reason of the difference. It is also unclear that the empirical scaling for ITER has little dependences on α_P, α_T. The reasonable scaling of the bootstrap current with a finite aspect ratio needs further efforts. It might be better to start with the numerical fit for a large aspect ratio.

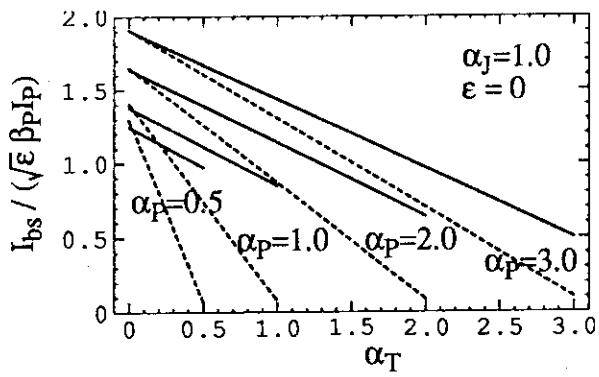

Fig.7 Comparison of α_P-, α_T- dependences of bootstrap currents with a large aspect ratio limit. The solid lines are the results from the empirical fit of equilibria with various aspect ratios [6], and the dashed lines are numerical results with an infinitely large aspect ratio.

5. Summary

The bootstrap current for a tokamak with a large aspect ratio limit is studied, placing emphasis on current density profiles, which should have reasonable shapes. The results can be summarized as follows.

(1) The bootstrap current for a tokamak with a large aspect ratio can be easily calculated with the use of a proposed fitting expression.

(2) The profile of the bootstrap current, having intrinsically a hollow profile, is mainly dependent on the pressure profile, and the peak of the bootstrap current density appears rather near the plasma axis for a large α_P, and with decreasing α_P the peak moves to the plasma edge and for $\alpha_P \leq 1.0$ the peak is at the plasma boundary.

(3) The profile of the external source current density is investigated for various profiles of pressure (α_P) and total current (α_J). For the upper-left space of the α_P-α_J plane the minimum of the external current density becomes negative near the plasma edge. In such a case the external source current have to be driven in both directions, i.e., the current drive system could be complicated.

(4) In the space of the lower-right corner of the α_P-α_J plane the external source current density is positive, and it should be selected for the design point. However with increasing I_{bs}/I_P, the negative external source current density appears again, where the bootstrap current density is greater than the total current density somewhere between the plasma axis and edge.

(5) The fraction of the negative external source current is also evaluated in the α_P-α_J plane. For a combination of small α_P and large α_J the fraction of the negative current reaches easily half of the bootstrap current.

(6) The value of $\sqrt{\varepsilon}\beta_P$ necessary to generate the given bootstrap current, is also evaluated in the α_P-α_J plane. In the lower-right corner of the α_P-α_J plane, is a favourable space for generating the large bootstrap current for a small poloidal beta.

(7) Generally speaking, the combination of the larger α_P and smaller α_J is favourable for utilization of bootstrap current in tokamaks.

The scaling of the bootstrap current is reviewed to some extent. Further careful studies are necessary for deriving a reasonable scaling. Especially the effect of the finite aspect ratio should be taken into consideration. In near future we will report somewhere a useful scaling of the bootstrap current with a finite aspect ratio.

Acknowledgements

The authors would like to express appreciation to Drs. M. Azumi and K. Tani for stimulated discussions on the subject. One of the authors (T. T.) expresses his sincere thanks to Dr. V. Pustovitov of Kurchatov Institute for his fruitful suggestion.

5. Summary

The bootstrap current for a tokamak with a large aspect ratio limit is studied, placing emphasis on current density profiles, which should have reasonable shapes. The results can be summarized as follows.

(1) The bootstrap current for a tokamak with a large aspect ratio can be easily calculated with the use of a proposed fitting expression.

(2) The profile of the bootstrap current, having intrinsically a hollow profile, is mainly dependent on the pressure profile, and the peak of the bootstrap current density appears rather near the plasma axis for a large α_P, and with decreasing α_P the peak moves to the plasma edge and for $\alpha_P \leq 1.0$ the peak is at the plasma boundary.

(3) The profile of the external source current density is investigated for various profiles of pressure (α_P) and total current (α_J). For the upper-left space of the α_P-α_J plane the minimum of the external current density becomes negative near the plasma edge. In such a case the external source current have to be driven in both directions, i.e., the current drive system could be complicated.

(4) In the space of the lower-right corner of the α_P-α_J plane the external source current density is positive, and it should be selected for the design point. However with increasing I_{bs}/I_P, the negative external source current density appears again, where the bootstrap current density is greater than the total current density somewhere between the plasma axis and edge.

(5) The fraction of the negative external source current is also evaluated in the α_P-α_J plane. For a combination of small α_P and large α_J the fraction of the negative current reaches easily half of the bootstrap current.

(6) The value of $\sqrt{\varepsilon}\beta_P$ necessary to generate the given bootstrap current, is also evaluated in the α_P-α_J plane. In the lower-right corner of the α_P-α_J plane, is a favourable space for generating the large bootstrap current for a small poloidal beta.

(7) Generally speaking, the combination of the larger α_P and smaller α_J is favourable for utilization of bootstrap current in tokamaks.

The scaling of the bootstrap current is reviewed to some extent. Further careful studies are necessary for deriving a reasonable scaling. Especially the effect of the finite aspect ratio should be taken into consideration. In near future we will report somewhere a useful scaling of the bootstrap current with a finite aspect ratio.

Acknowledgements

The authors would like to express appreciation to Drs. M. Azumi and K. Tani for stimulated discussions on the subject. One of the authors (T. T.) expresses his sincere thanks to Dr. V. Pustovitov of Kurchatov Institute for his fruitful suggestion.

References

[1] ITER Conceptual Design Report, IAEA/ITER/DS/18, ITER Documentation Series, IAEA, Vienna (1991).
[2] Y. Seki and SSTR Design Team, "The Steady State Tokamak Reactor (SSTR)", 13th Int. Conf. on Plasma Phys. and Contr. Nucl. Fusion Res., IAEA-CN-53/G-1-2 (1990).
[3] R.W. Conn, F. Najmabadi, and The ARIES Team, "A Steady-State, First-Stability Tokamak Reactor with Enhanced Safety and Environmental Features", 13th Int. Conf. on Plasma Phys. and Contr. Nucl. Fusion Res., IAEA-CN-53/H-1-4 (1990).
[4] ITER Physics Design Guidelines:1989, IAEA/ITER/DS/10, ITER Documentation Series, IAEA, Vienna (1990).
[5] ITER Physics, IAEA/ITER/DS/21, ITER Documentation Series, IAEA, Vienna (1991).
[6] H.R. Wilson, Nuclear Fusion 32 (1992) 257.
[7] M.N. Rosenbluth, R.D. Hazeltine, F.L. Hinton, Physics Fluids 15 (1972) 116.